ECS Journal of Solid State
Science and Technology

OPEN ACCESS

Electronic Properties of Ga_2O_3 Polymorphs

To cite this article: John L. Lyons 2019 *ECS J. Solid State Sci. Technol.* **8** Q3226

JSS Focus Issue on Gallium Oxide Based Materials and Devices

Electronic Properties of Ga_2O_3 Polymorphs

John L. Lyons [z]

Center for Computational Materials Science, U.S. Naval Research Laboratory, Washington, DC 20375, USA

Ga_2O_3 is an ultra-wide-band-gap semiconductor especially promising for power electronic applications. One advantage of this material is its ability to exist in different phases, which may add flexibility to device design, namely through polarization engineering of two-dimensional electron gases. Although much is known about monoclinic β-Ga_2O_3, much less is known about many basic electronic properties of other phases. In this work, four of the most common phases of Ga_2O_3 (α, β, κ, and ϵ) are investigated with first-principles calculations based on hybrid density functional theory. The structural and electronic properties of each phase are compared, and band offsets between the phases and other common wide-band-gap semiconductors are determined. All four phases of Ga_2O_3 are found to exhibit self-trapping holes, large Mg acceptor ionization energies, deep oxygen vacancy donor levels, and low-lying valence-band maxima. In addition, all phases have large valence-band offsets but small or modest conduction-band offsets with GaN, SiC, and Si. With AlN and diamond, all Ga_2O_3 phases have large conduction-band and valence-band offsets.
 [DOI: 10.1149/2.0331907jss]

Manuscript received March 13, 2019. Published May 14, 2019. *This paper is part of the JSS Focus Issue on Gallium Oxide Based Materials and Devices.*

The wide bandgap, large breakdown voltage, high device figures of merit, and substrate availability make Ga_2O_3 a tantalizing material for power electronics applications.[1–4] Steady progress has been made in Ga_2O_3-based devices, for instance the demonstration of vertical transistors with breakdown voltages over 1 kV,[5] transistors with power added efficiency of 12% at 1 GHz,[6] modulation-doped field effect transistors with sheet charge densities of $1.2 \cdot 10^{13}$ cm^{-3},[7] and enhancement-mode transistors with high breakdown voltages.[4]

The polymorphism exhibited by Ga_2O_3 may spur further breakthroughs in gallium-oxide-based power electronics. Nearly all Ga_2O_3-containing devices utilize the monoclinic β phase, the most stable and best-characterized polymorph.[8,9] However, other phases of Ga_2O_3 have also received attention due to potentially favorable growth characteristics, and to the possibility of polarization engineering made possible by the polar nature of their crystal structures.[10–12] In principle, this polarization could be utilized to produce two-dimensional electron gases (2DEGs) in analogy with GaN/AlN-based transistors.[13] Although α-Ga_2O_3 is not usually discussed in the context of polarization, its structure is analogous to the ground-state corundum phase of Al_2O_3. Thus understanding α-Ga_2O_3 is necessary for understanding the characteristics of Ga_2O_3-Al_2O_3 alloys[14] that will be crucial for gallium oxide heterostructures.[15]

Theoretical studies have revealed some properties of different Ga_2O_3 phases .[9,13,14,16] Early work examined structural properties, and reported that the β phase was most stable (although the ϵ phase was found to be stable above 1600 K).[9] More recent work has established the polarization properties of the ϵ and κ phases.[13,16] Although band offsets were recently reported for the α and β phases,[14] they have apparently not been reported for the ϵ or κ phases. Furthermore, although hole trapping and acceptor properties have been discussed in the theoretical literature for the β phase of Ga_2O_3,[17–20] much less is known about these properties in other phases.

In this work, the basic electrical properties of the α, β, κ, and ϵ phases of Ga_2O_3 are calculated and compared. In addition to lattice parameters and band gaps, the stability of self-trapped holes and Mg acceptor ionization energies are also calculated. Band offsets are determined and compared with the wide-band-gap nitride semiconductors, diamond, Si, and with the 4H and 6H phases of SiC, all of which may be useful when incorporated into Ga_2O_3-containing devices.

The properties of Ga_2O_3 phases are examined here using hybrid density functional theory, which has been shown to accurately describe the band structures of wide-band-gap semiconductors as well as deep defect behavior within them.[18,19,21–23] These calculations are based on generalized Kohn-Sham theory[24,25] and use the screened hybrid functional of Heyd-Scuseria-Ernzerhof (HSE)[26] with the projector-augmented wave method,[27] as implemented in VASP.[28] The fraction of Hartree-Fock exchange for all phases is set to 0.32, yielding a bandgap (4.87 eV)[14] in close agreement with experiment (4.90 eV)[29] for β-Ga_2O_3, the best characterized phase of gallium oxide. For consistency, these parameters are also applied to the other three polymorphs. Encouragingly, the calculated bandgap for ϵ-Ga_2O_3 of 4.48 eV falls within the 4.4-4.6 eV range of band gaps reported from experiments.[30,31] Also, the bandgap of α-Ga_2O_3 is consistent with previous calculations,[14] and is consistent with the larger 5.3 eV bandgap observed in optical studies.[32]

400 eV plane-wave cutoffs and two special k-points are used for all supercell calculations. For calculations of α-Ga_2O_3, β-Ga_2O_3, and ϵ-Ga_2O_3, 120-atom supercells were employed, while for κ-Ga_2O_3, an 80-atom supercell was used. In each case, spin polarization is explicitly taken into account for the neutral charge states of impurities and for polarons. Ga 3*d* electrons were treated in the core, as their inclusion has a negligible effect on defect formation energies.[33] Calculations of defect thermodynamic transition levels are performed in accordance with the standard formalism,[21] and consistently with previous calculations in Ref. 19. The calculated lattice parameters for each phase of Ga_2O_3 are shown in Table I. The lattice parameters are in good agreement with previous theoretical studies[9,14,16,33] and experimental observations.[34] Some controversy exists over the structural assignments for ϵ- and κ-Ga_2O_3.[11,16,35] In this study, the structure of ϵ-Ga_2O_3 is adopted from Ref. 34, and κ-Ga_2O_3 is adopted from Ref. 16.

Different coordinations exist for both Ga and O atoms in Ga_2O_3 polymorphs. For the sake of comparison, the same coordination is

Table I. Calculated lattice parameters, direct band gaps, hole self-trapping energies (E_{ST}), and Mg_{Ga} acceptor ionization energies for the four phases of Ga_2O_3 considered.

phase	*a* (Å)	*b* (Å)	*c* (Å)	bandgap (eV)	E_{ST} (eV)	Mg_{Ga} (0/−) (eV)
α	4.94	–	13.30	5.57	0.51	1.11
β	12.16	3.03	5.79	4.87	0.53	1.36
ϵ	2.99	14.38	9.20	4.48	0.79	1.45
κ	5.04	8.61	9.19	4.84	0.87	1.46

[z]E-mail: john.lyons@nrl.navy.mil

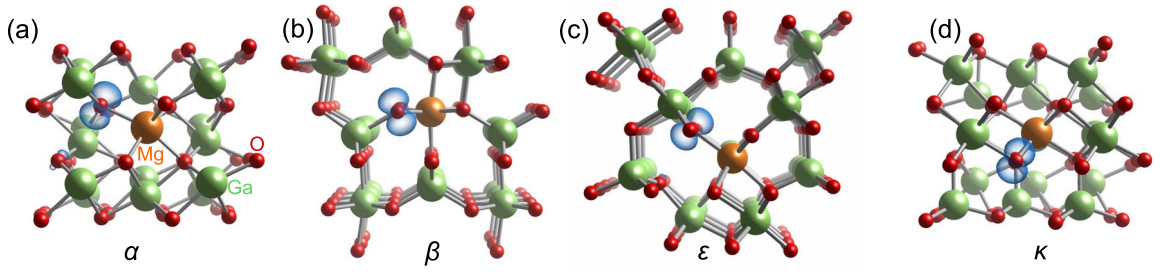

Figure 1. Spin densities of Mg^0_{Ga} acceptors in the four different Ga_2O_3 polymorphs studied here: (a) α, (b) β, (c) ϵ, and (d) κ. Isosurfaces are set to 5% of the maximum in each case.

utilized for each defect center in each phase where possible. Mg_{Ga} is chosen to substitute for 6-fold coordinated Ga in each phase, as this configuration is the lowest in energy for β-Ga_2O_3.[19] For the oxygen vacancy (V_O), the 4-fold coordinated O sites are chosen, since it is the lowest-energy configuration for V_O^{2+} in β-Ga_2O_3.[33] Hole self-trapping energies (E_{ST}; as defined in Ref. 17) are reported for whichever site exhibits the largest E_{ST}. Band alignments between the different phases of Ga_2O_3 and other wide-band semiconductors were calculated using surface-slab calculations with nonpolar orientations. This approach allows the electrostatic potential within each material to be referenced to vacuum, and provides natural band alignments that avoid strain or lattice mismatch effects.[36,37] For each surface calculation, supercells using at least 15 Å of material were used, together with at least 15 Å of vacuum to avoid spurious interactions. All atoms within 5 Å of the surface were allowed to relax.

Previous calculations indicated that holes spontaneously localize in the β phase of Ga_2O_3;[17] in this work holes are found to self trap in all phases of Ga_2O_3. The E_{ST} of these hole polarons vary between 0.5–0.9 eV, and are listed in Table I. This indicates that in every phase of Ga_2O_3 holes prefer to spontaneously localize onto single O sites, as opposed to being delocalized free holes, even in the absence of any defect or impurity species. In all but one phase holes prefer to trap onto three-fold-coordinated oxygen sites. The exception is the α phase, which does not contain such sites, thus holes can only localize onto a four-fold O site. α-Ga_2O_3 has the lowest E_{ST} of all phases studied here, while κ-Ga_2O_3 has the highest. Should the Fermi level approach the E_{ST} level within Ga_2O_3, the polaron will act as a hole trap as has been previously predicted for AlN.[38]

Cation-site acceptors such as Mg_{Ga} have been shown to act as "polaronic" acceptors in Ga_2O_3,[18,19] meaning that they trap holes onto nearest-neighbor O sites and act as deep acceptors. Because of the similarities in hole-trapping behavior found for all phases of Ga_2O_3, it is expected that the behavior of cation-site acceptors should be consistent in these compounds. This is confirmed by examining the ionization energies [equivalent to the acceptor's (0/−) thermodynamic transition level] of the Mg_{Ga} acceptor in each Ga_2O_3 phase, which are shown in Table I. These energies range from 1.1–1.5 eV, indicating that Mg dopants will be deep in every phase of Ga_2O_3. Furthermore, these energies exhibit the same pattern as the self-trapped holes, with α-Ga_2O_3 having the smallest Mg_{Ga} ionization energy and κ-Ga_2O_3 having the highest.

In Fig. 1, isosurfaces of the spin densities for Mg^0_{Ga} are shown for each phase of gallium oxide. In all cases, a highly localized hole is trapped at an O site adjacent to Mg_{Ga}. As was the case for hole polarons, Mg_{Ga} traps holes onto a three-fold-coordinated O site for all phases except for α-Ga_2O_3, where Mg_{Ga} traps a hole onto an adjacent four-fold site. Isosurface plots of the self-trapped holes (not shown) in each phase look nearly identical to those shown in Fig. 1, albeit with the absence of the Mg_{Ga} impurity.

The behavior of V_O, known to be a negative-U donor in β-Ga_2O_3,[33] serves as another means for comparing the properties of gallium oxide phases. The negative-U nature of V_O derives from the fact that the 1+ charge state is not stable, and only V_O^2+ and V_O^0 will be present in thermal equilibrium. This same behavior is also observed for V_O in each phase of Ga_2O_3. As shown in Fig. 2, V_O is also a deep donor in each phase, and the (2+/0) transition level lies between 1.5–2.1 eV below the CBM of all phases of Ga_2O_3.

The results for the thermodynamic transition levels self-trapped holes, Mg_{Ga} acceptors and V_O donors are incorporated into Fig. 2, which also shows band offsets between Ga_2O_3 phases as well as GaN, AlN, SiC, Si, and diamond. Note that due to the large Stokes shifts predicted for Ga_2O_3 defects, optical transition levels will vary considerably from the thermodynamic transition levels.[17,39] Note also that all band edge positions are referenced to the valence band maximum (VBM) of GaN, which is set to 0 eV in Fig. 2. As would be expected due to the shared O 2p character of the valence band and of the polaronic states, the positions of Mg_{Ga} acceptor levels (and self-trapped holes) roughly follow the position of the gallium oxide VBM. The positions of the V_O donor levels roughly track each oxide CBM, as is expected since their defect states derive from the Ga s orbitals that comprise the conduction band. The overall variation in the absolute positions of the CBM and VBM of the gallium oxide phases is 0.9 eV or less, which is also roughly the level of variation in the band gaps, as shown in Table I. In comparison with the other semiconductors shown in Fig. 2, the Ga_2O_3 phases have much lower-lying VBM.

All Ga_2O_3 phases have sizeable valence-band offsets (VBO) with GaN. The smallest VBO (1.1 eV) occurs for GaN/ϵ-Ga_2O_3; all others are 1.7 eV or larger. The conduction band offsets (CBO) between GaN and Ga_2O_3 phases are much smaller in comparison; none are larger than 0.5 eV. The calculated offsets for β-Ga_2O_3/GaN (VBO = 1.7 eV, CBO = 0.3 eV) are in good agreement with an X-ray photoelectron spectroscopy (XPS) study[40] that reported a VBO of 1.4 eV and a CBO of 0.1 eV for the β-Ga_2O_3/GaN heterostructure.

In contrast to GaN, the CBOs between Ga_2O_3 and AlN are much larger, and exceed 2 eV for all phases. The calculated VBOs are all larger than 1 eV. This result conflicts with some recent XPS studies that report VBOs of −0.1 eV for plasma-assisted atomic-layer deposited (ALD) AlN and 0.7 eV for thermal ALD AlN in one study[12] and 0.6 eV in another[41] (giving resulting CBOs between 0.6 and 1.8 eV.[12,41]). However, it has been noted[12] that oxygen incorporation into AlN films may explain the large discrepancies between these values, which might also explain why they strongly deviate from the calculated offsets.

The calculated band offsets between diamond and the Ga_2O_3 phases are similar to those of AlN, featuring large CBO and VBO. Both phases of SiC have small CBO with all Ga_2O_3 phases, but have VBO that are greater than 1 eV in each case.

In the case of Si, all phases have substantial VBO that are all in excess of 2.5 eV. The calculated β-Ga_2O_3/Si VBO of 3.4 eV is in good agreement with two XPS studies that report a 3.5 eV offset.[42,43] However, for CBOs with Si there is more variation between the Ga_2O_3 phases. The CBOs are small for κ-Ga_2O_3/Si (0.2 eV) and β-Ga_2O_3/Si (0.4 eV). However, those for ϵ-Ga_2O_3/Si (0.8 eV) and α-Ga_2O_3/Si (1.1 eV) are more substantial.

In summary, hybrid functional calculations indicate that the α, β, κ, and ϵ phases of Ga_2O_3 exhibit broadly similar electronic properties. In all phases, holes self trap as polarons, meaning that free holes will not

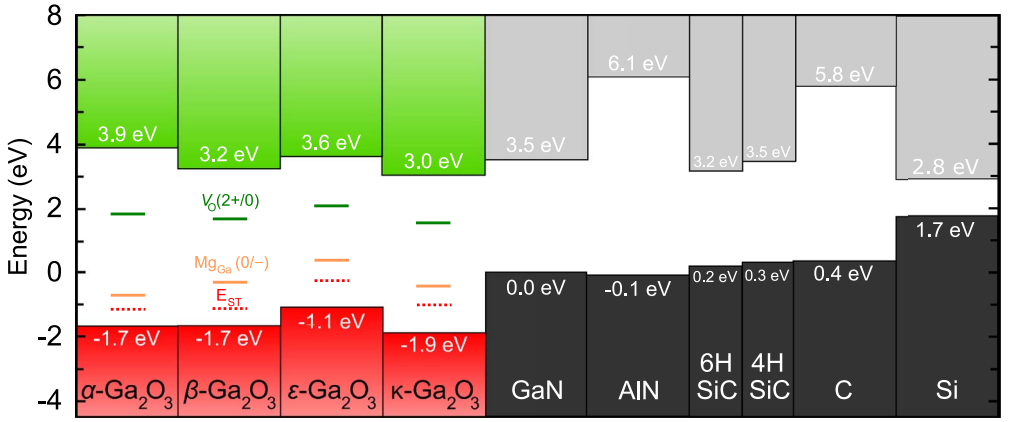

Figure 2. Band offsets between the α, β, ϵ, and κ phases of Ga_2O_3 together with those of GaN, AlN, 4H-SiC, 6H-SiC, Si, and diamond. The dotted red lines in the oxide band gaps indicate the hole self-trapping energy relative to the VBM of the Ga_2O_3 phases. The orange lines indicate the ionization energies of Mg_{Ga} acceptors in each phase, while the green lines indicate the V_O (2+/0) donor levels. Values in white indicate the energetic position of each band maximum or minimum.

be stable. This hole trapping also affects the properties of acceptors in these polymorphs, and Mg_{Ga} acceptors have large ionization energies in each phase. A comparison of band offsets indicates that all phases have low-lying VBM, 1 eV or more below that of GaN, AlN, SiC, Si and diamond. Furthermore, while all phases have CBM in the vicinity of those of GaN, SiC, and Si, they have substantial conduction band offsets with AlN and diamond.

Acknowledgments

V. D. Wheeler and D. J. Meyer are thanked for helpful discussions. This work was supported by the Office of Naval Research (ONR) Basic Research Program, and computations were performed at the DoD Major Shared Resource Center at AFRL.

ORCID

John L. Lyons https://orcid.org/0000-0001-8023-3055

References

1. M. Higashiwaki, K. Sasaki, H. Murakami, Y. Kumagai, A. Koukitu, A. Kuramata, T. Masui, and S. Yamakoshi, *Semicond. Sci. Technol.*, **31**, 034001 (2016).
2. J. Y. Tsao, S. Chowdhury, M. A. Hollis, D. Jena, N. M. Johnson, K. A. Jones, R. J. Kaplar, S. Rajan, C. G. Van de Walle, E. Bellotti, C. L. Chua, R. Collazo, M. E. Coltrin, J. A. Cooper, K. R. Evans, S. Graham, T. A. Grotjohn, E. R. Heller, M. Higashiwaki, M. S. Islam, P. W. Juodawlkis, M. A. Khan, A. D. Koehler, J. H. Leach, U. K. Mishra, R. J. Nemanich, R. C. N. Pilawa-Podgurski, J. B. Shealy, Z. Sitar, M. J. Tadjer, A. F. Witulski, M. Wraback, and J. A. Simmons, *Adv. Elec. Mat.*, **4**, 1600501 (2017).
3. M. A. Mastro, A. Kuramata, J. C. Calkins, J. Kim, F. Ren, and S. J. Pearton, *ECS J. Sol. State Sci. and Tech.*, **6**, P356 (2017).
4. K. D. Chabak, J. P. McCandless, N. A. Moser, A. J. Green, K. Mahalingam, A. Crespo, N. Hendricks, B. M. Howe, S. E. Tetlak, K. Leedy, R. C. Fitch, D. Wakimoto, K. Sasaki, A. Kuramata, and G. H. Jessen, *IEEE Electron Device Letters*, **39**, 67 (2018).
5. Z. Hu, K. Nomoto, W. Li, N. Tanen, K. Sasaki, A. Kuramata, T. Nakamura, D. Jena, and H. G. Xing, *IEEE Elec. Dev. Lett.*, **39**, 869 (2018).
6. M. Singh, M. A. Casbon, M. J. Uren, J. W. Pomeroy, S. Dalcanale, S. Karboyan, P. J. Tasker, M. H. Wong, K. Sasaki, A. Kuramata, S. Yamakoshi, M. Higashiwaki, and M. Kuball, *IEEE Electron. Dev. Lett.*, **39**, 1572 (2018).
7. E. Ahmadi, O. S. Koksaldi, X. Zheng, T. Mates, Y. Oshima, U. K. Mishra, and J. S. Speck, *Appl. Phys. Exp.*, **10**, 071101 (2017).
8. R. Roy, V. G. Hill, and E. F. Osborn, *Journal of the American Chemical Society*, **74**, 719 (1952).
9. S. Yoshioka, H. Hayashi, A. Kuwabara, F. Oba, K. Matsunaga, and I. Tanaka, *J. Phys: Condens. Matt.*, **19**, 346211 (2007).
10. Y. Oshima, E. G. VÃllora, Y. Matsushita, S. Yamamoto, and K. Shimamura, *J. Appl. Phys.*, **118**, 085301 (2015).
11. F. Mezzadri, G. Calestani, F. Boschi, D. Delmonte, M. Bosi, and R. Fornari, *Inorg. Chem.*, **55**, 12079 (2016).
12. Z. Chen, Z. Li, Y. Zhuo, W. Chen, X. Ma, Y. Pei, and G. Wang, *Appl. Phys. Expr.*, **11** (2018).
13. M. B. Maccioni and V. Fiorentini, *Appl. Phys. Expr.*, **9**, 041102 (2016).
14. H. Peelaers, J. B. Varley, J. S. Speck, and C. G. Van de Walle, *Appl. Phys. Lett.*, **112**, 242101 (2018).
15. P. Vogt, A. Mauze, F. Wu, B. Bonef, and J. S. Speck, *Applied Physics Express*, **11**, 115503 (2018).
16. J. Kim, D. Tahara, Y. Miura, and B. G. Kim, *Appl. Phys. Express*, **11**, 061101 (2018).
17. J. B. Varley, A. Janotti, C. Franchini, and C. G. Van de Walle, *Phys. Rev. B*, **85**, 081109 (2012).
18. A. Kyrtsos, M. Matsubara, and E. Bellotti, *Appl. Phys. Lett.*, **112**, 032108 (2018).
19. J. L. Lyons, *Semicon. Sci. Tech.*, **33**, 05LT02 (2018).
20. Q. D. Ho, T. Frauenheim, and P. Dek, *Journal of Applied Physics*, **124**, 145702 (2018).
21. C. Freysoldt, B. Grabowski, T. Hickel, J. Neugebauer, G. Kresse, A. Janotti, and C. G. Van de Walle, *Rev. Mod. Phys.*, **86**, 253 (2014).
22. M. E. Ingebrigtsen, J. B. Varley, A. Y. Kuznetsov, B. G. Svensson, G. Alfieri, A. Mihaila, U. Badstübner, and L. Vines, *Applied Physics Letters*, **112**, 042104 (2018).
23. A. Carvalho, A. Alkauskas, A. Pasquarello, A. K. Tagantsev, and N. Setter, *Phys. Rev. B*, **80**, 195205 (2009).
24. P. Hohenberg and W. Kohn, *Phys. Rev.*, **136**, B864 (1964).
25. W. Kohn and L. Sham, *Phys. Rev.*, **140**, A1133 (1965).
26. J. Heyd, G. E. Scuseria, and M. Ernzerhof, *J. Chem. Phys.*, **118**, 8207 (2003).
27. P. E. Blöchl, *Phys. Rev. B*, **50**, 17953 (1994).
28. G. Kresse and J. Joubert, *Phys. Rev. B*, **59**, 1758 (1999).
29. M. Orita, H. Ohta, and M. Hirano, *Appl. Phys. Lett.*, **77**, 4166 (2000).
30. M. Pavesi, F. Fabbri, F. Boschi, G. Piacentini, A. Baraldi, M. Bosi, E. Gombia, A. Parisini, and R. Fornari, *Materials Chemistry and Physics*, **205**, 502 (2018).
31. M. Mulazzi, F. Reichmann, A. Becker, W. M. Klesse, P. Alippi, V. Fiorentini, A. Parisini, M. Bosi, and R. Fornari, *APL Materials*, **7**, 022522 (2019).
32. D. Shinohara and S. Fujita, *Japn. J. Appl. Phys.*, **947**, 7311 (2008).
33. J. B. Varley, J. R. Weber, A. Janotti, and C. G. Van de Walle, *Applied Physics Letters*, **97**, 142106 (2010).
34. H. Y. Playford, A. C. Hannon, E. R. Barney, and R. I. Walton, *Chem. Eur. J.*, **19**, 2803 (2013).
35. I. Cora, F. Mezzadri, F. Boschi, M. Bosi, M. aploviov, G. Calestani, I. Ddony, B. Pcza, and R. Fornari, *Cryst. Eng. Comm.*, **19**, 1509 (2017).
36. A. Franciosi and C. G. Van de Walle, *Surf. Sci. Rep.*, **25**, 1 (1996).
37. P. G. Moses and C. G. Van de Walle, *Applied Physics Letters*, **96**, 021908 (2010).
38. J. L. Lyons, K. Krishnaswamy, L. Gordon, A. Janotti, and C. G. Van de Walle, *IEEE Electron. Dev. Lett.*, **37**, 154 (2016).
39. C. Freysoldt, B. Grabowski, T. Hickel, J. Neugebauer, G. Kresse, A. Janotti, and C. G. Van de Walle, *Rev. Mod. Phys.*, **86**, 253 (2014).
40. W. Wei, Z. Qin, S. Fan, Z. Li, K. Shi, Q. Zhu, and G. Zhang, *Nanoscale Res. Lett.*, **7**, 562 (2012).
41. H. Sun, C. G. Torres Castanedo, K. Liu, K.-H. Li, W. Guo, R. Lin, X. Liu, J. Li, and X. Li, *Applied Physics Letters*, **111**, 162105 (2017).
42. Z. Chen, K. Nishihagi, X. Wang, K. Saito, T. Tanaka, M. Nishio, M. Arita, and Q. Guo, *Applied Physics Letters*, **109**, 102106 (2016).
43. J. T. Gibbon, L. Jones, J. W. Roberts, M. Althobaiti, P. R. Chalker, I. Z. Mitrovic, and V. R. Dhanak, *AIP Advances*, **8**, 065011 (2018).